Asymmetry in the Indian Summer Monsoon Rainfall response to two types of La Niña evolution

Satyaban B. Ratna[1]*, Tanu Sharma[1], Arti Bandgar[1], O. P. Sreejith[1], D. S. Pai[2], M. Rajeevan[3], K. S. Hosalikar[1] and M. Mohapatra[4]

[1] Climate Research and Services, India Meteorological Department, Pune, India

[2] The Institute for Climate Change Studies (ICCS), Kottayam, Kerala, India

[3] National Centre for Earth Science Studies, Thiruvananthapuram, Kerala, India

[4]India Meteorological Department, New Delhi, India

***Correspondence to:**

Satyaban B. Ratna

E-Mail: satyaban.ratna@imd.gov.in

ORCID

Satyaban B. Ratna https://orcid.org/0000-0001-8780-8165

Tanu Sharma https://orcid.org/0000-0002-2963-7174

Arti Bandgar

O. P. Sreejith https://orcid.org/0000-0002-3928-056X

D. S. Pai https://orcid.org/0000-0001-8392-5735

M. Rajeevan https://orcid.org/0000-0002-3000-2459

K. S. Hosalikar https://orcid.org/0009-0003-8941-3097

M. Mohapatra

Key Points:

- Two types of La Niña are distinguished for the June-September season based on whether they evolved from El Niño or La Niña in boreal winter.
- India receives more (less) summer monsoon rainfall when La Niña evolves from the El Niño (La Niña) in the previous boreal winter season.
- The difference in rainfall is linked to changes in large-scale atmospheric circulation over the tropical Indian and Pacific Oceans.

Abstract

This study attempts to understand the asymmetry in the Indian Summer Monsoon Rainfall (ISMR) response to two types of La Niña whether they evolved from El Niño or La Niña in the previous boreal winter season. It was seen that nine La Niña years during the monsoon season were preceded by El Niño (hereafter ELLA) whereas eight were preceded by La Niña (hereafter LALA) during the period 1961-2021. India received more rainfall during the ELLA years as compared to the LALA years, linked to the difference in the Sea Surface Temperature (SST) and large-scale atmospheric circulation anomalies over the tropical Pacific and Indian oceans. Based on the strength and patterns of the cold SST anomaly and shift in the Walker circulation over the equatorial Pacific Ocean, the enhanced (weakened) convection over the Indian landmass during the ELLA (LALA) years, contributed to more (less) rainfall over India.

Plain language summary

A well-established inverse relationship between the El Niño-Southern Oscillation (ENSO) in the equatorial Pacific Ocean and the Indian Summer Monsoon Rainfall (ISMR) is known but their relationship is not always linear. It is also known that the evolution of La Niña events is not always the same and hence their effect on the ISMR. Two types of La Niña events during the boreal summer monsoon season are identified with respect to their evolution, whether there was an El Niño or a La Niña during the previous boreal winter season, and they are termed ELLA and LALA events, respectively. India receives higher ISMR during the ELLA years compared to the LALA years due to the patterns and strength of SST anomaly and associated large-scale atmospheric circulation over the tropical Pacific and Indian Oceans. The low-level convergence and enhanced convection over the Indian landmass during ELLA years contribute to higher rainfall over India. However, the low-level convergence and convection weakens over Indian region during LALA years, reduces the rainfall over India. This study will be helpful for understanding the rainfall variability over India based on the evolution of the SST anomaly in the equatorial Pacific Ocean.

Keywords: Indian Summer Monsoon Rainfall, La Niña, ENSO evolution, Indo-Pacific Ocean, Sea Surface Temperature, Walker circulation

1. Introduction

The Indian Summer Monsoon Rainfall (ISMR) or south-west monsoon from June to September (JJAS) season, is a land-atmosphere-ocean coupled system that contributes about 70 % of the annual rainfall over the Indian landmass (Shukla and Haung, 2016). The ISMR plays a crucial role in the agricultural and socio-economical structure of the subcontinent (Gadgil and Gadgil, 2006). The ISMR has a large range of temporal (from diurnal to multi-decadal) and spatial variability, which makes its prediction a challenge (Goswami, 2004). Many studies found that interannual variation of ISMR is linked to the changing boundary conditions at the local level as well as the remote teleconnections such as the Indian Ocean Dipole (IOD), Equatorial Indian Ocean Oscillation (EQUINOO), North Atlantic Oscillation (NAO), Pacific Decadal Oscillation (PDO), snow cover over Eurasia, Meridional Surface Air Temperature Anomaly Gradient Index (MTAGI) across Eurasia and El Niño Southern Oscillation (ENSO) (Kumar et al., 1999; Saji et al., 1999; Gillett et al., 2003; Pai, 2004; Gadgil et al., 2007; Hrudya et al., 2021; Ratna et al., 2021).

The ENSO is an ocean-atmospheric coupled phenomenon having a quasi-periodic nature. The typical life cycle of ENSO consists of its growth in boreal spring or summer, reaching its peak in winter, and decay in the following spring (Jin et al., 1994; Tziperman et al., 1994; Iwakiri and Watanabe, 2021). The ENSO is the most prominent forcing on the ISMR which explains almost 29% of its total interannual variability (Chakraborty and Singhai, 2021). The ISMR shows a negative correlation with the simultaneous central-equatorial Pacific (Niño 3.4 region: area over 5 °S-5 °N and 170 °W-120 °W) sea surface temperature (SST) anomalies. As a result of that, the La Niña (El Niño) event enhances (weakens) the ISMR through the displacement of the Walker circulation (Sikka and Gadgil, 1980; Webster and Yang, 1992; Kirtman and Shukla, 2000). However, every monsoon drought and flood is not associated with the ENSO condition (Roxy and Chaithra, 2018).

The oscillatory behavior of ENSO is inconsistent with respect to its temporal evolution and the transition among its phases such as El Niño, La Niña, and Neutral (Neelin et al., 2000; Timmermann et al., 2018). According to the study by Dommenget et al (2013), all the El Niño and La Niña events are not the same as there is a non-linearity in the amplitude, spatial pattern, and time evolution of these events. A study by Cole (2002) discussed that generally, the El Niño phase ends quickly whereas the La Niña phase lasts longer (multi-year La Niña). It is found in

observations that after a strong El Niño, the probability of occurrence of a multi-year La Niña is high and this multi-year La Niña events are occurring more frequently in recent decades (Dommenget et al., 2013).

As every ENSO event is not the same in terms of evolution, spread and intensity; its impact on the ISMR is asymmetric. This made us curious to study how the different evolutions of the cold phase of the ENSO (La Niña) influence the ISMR differently. We identified two types of La Niña events, where the La Niña events are preceded by El Niño (ELLA) in the previous boreal winter and the other one is La Niña preceded by La Niña (LALA) in the previous boreal winter; during the period 1961-2021. The objective of this study is (i) to understand the changes in the SST and the spatial pattern of rainfall over India with respect to these two types of La Niña events (ELLA and LALA); (ii) to understand the dynamics in terms of large-scale circulation patterns for two types of La Niña that contributes to rainfall anomalies over India. The paper is organized as follows: Section 2 describes the data and the methodology applied for this study. Section 3 is dedicated to the results and discussions; section 4 summarizes the findings of the work.

2. Data and Methodology

2.1 Data

The Oceanic Niño Index (ONI) from 1961 to 2021, is taken from the National Weather Service website *https://origin.cpc.ncep.noaa.gov/products/analysis_monitoring/ensostuff/ONI_v5.php* NOAA. ONI is one of the primary indicators for the oceanic component of the ENSO (3-month running mean of ERSST.v5 SST anomalies in the Niño 3.4 region), based on a centered 30-year base period. The rainfall dataset used for the study is the high spatial resolution (0.25 ° x 0.25 °) gridded monthly data for the Indian region, for the period 1901-2021, prepared by the India Meteorological Department (Pai et al., 2014). For SST, the NOAA Extended Reconstructed Sea monthly Surface Temperature (ERSST) dataset (Huang et al., 2017) downloaded from the website *https://psl.noaa.gov* which is available from January 1854 continuing to the present. For the horizontal wind velocity components (u and v) and vertical wind velocity (omega), we used monthly mean NCEP-NCAR Reanalysis 1 data (Kalnay et al., 1996) provided by the NOAA PSL, Boulder, Colorado, USA, from their website at *https://psl.noaa.gov* for the period January 1948 to April 2022.

2.2 Methodology

Defining ELLA and LALA events:

During the JJAS season, we considered those years as La Niña, for which the 3-month running mean of SST anomaly over the Niño 3.4 region (5 °N - 5 °S and 120 °W - 170 °W) is less than or equal to -0.5 °C during June-July-August (JJA) and July-August-September (JAS) seasons. Similarly, during the previous boreal winter, December-January-February (DJF) season, we considered those years as La Niña (El Niño), during which the 3-month mean Niño 3.4 region is less (more) than -0.5 °C (0.5 °C). Based on the time evolution of ONI, we categorize two types of La Niña events: 1). La Niña in the JJAS season is preceded by El Niño in the DJF season, as 'ELLA'. 2). La Niña in the JJAS season is preceded by La Niña in the DJF season, as 'LALA'. From 1961 to 2021, as per the above criteria, we found 17 years in which the La Niña event occurred during the JJAS season. Out of these 17 La Niña, 9 are identified as ELLA and 8 as LALA years. The list of ELLA years are 1964, 1970, 1973, 1988, 1998, 2007, 2010, 2016, and 2020.; and the list of LALA years are 1971, 1974, 1975, 1985, 1999, 2000, 2011, and 2021.

In order to understand how the two types of La Niña (ELLA and LALA) influence the ISMR, the composite analysis of rainfall, SST and winds are analyzed. All the anomalies are calculated with respect to the 1961-2020 climatology. We detrended the SST anomalies to remove the influence of basin-wide warming because of climate change. To understand the dynamical response of ELLA and LALA on ISMR, we examined the Walker circulations using zonal (u) components of the wind and the vertical velocity (ω), the velocity potential is also analyzed. The statistical significance of the composite anomalies is carried out with Student's t-test method.

3. Results and Discussion

3.1 Comparison of SST anomaly for ELLA and LALA events

The SST anomalies over the Indo-Pacific region play an important role in modulating spatial and temporal variability of the monsoon (Krishna Kumar et al., 2023; Cherchi et al., 2021). Figure 1(a) shows the time evolution of the ONI during the 3-month seasons for all the ELLA and LALA years. The figure shows the evolution of 17 La Niña years in which there are 9 ELLA years and 8 LALA years. The mean ONI values for ELLA (red) and LALA (blue) years are clearly showing the evolution of two types of La Niña events (Fig. 1a). It is clearly indicating that ELLA (LALA) events are evolving from a warm (cold) phase of ENSO in the boreal winter to La Niña in the

summer monsoon (JJAS) season (Fig. 1a, b). It was also observed that there is a difference in the mean intensity of ONI value for the JJAS season during the ELLA and LALA years. The mean intensity of La Niña during the summer monsoon season is higher for ELLA years as compared to LALA years. (Fig. 1a). To understand the evolution of ELLA and LALA events in detail, the composites of the detrended SST anomalies were plotted over the tropical Indo-Pacific Ocean. Figures 1(b) and 1(d) show the spatial pattern of the SST anomaly corresponding to ELLA during the DJF and the JJAS season respectively. In ELLA during the DJF season (Fig. 1b), positive and statistically significant SST anomalies are seen over the eastern Pacific Ocean, extending up to the central Pacific. The western Pacific Ocean is found to be relatively cold and positive SST anomalies are observed over the Indian Ocean. During the JJAS season (Fig. 1d), a clear cold tongue signature pattern of La Niña is seen with significant negative SST anomalies extended from the eastern coast up to the central Pacific Ocean. Significant positive SST anomalies are visible over the north Indian Ocean and the Maritime continent region. In terms of LALA composite during the DJF season (Fig. 1c) statistically significant cold SST anomalies are seen over the eastern Pacific Ocean, extending up to the central Pacific. The western Pacific Ocean is found to be relatively warmer. However, negative SST anomalies are observed over the north Indian Ocean. In the LALA composite during the JJAS season (Fig. 1e), a large spread of the significantly negative SST anomaly is seen over the eastern and central Pacific Ocean. At the same time, negative SST anomalies are present over the Indian Ocean. The comparison of SST anomalies between two types of La Niña during the JJAS season indicates that the spread of cold SST anomaly over the equatorial Pacific is narrow and strong during the ELLA composite whereas the spread of cold SST anomaly over the equatorial Pacific is relatively weak and wider in the LALA composite (Fig. 1d,e). The noticeable difference between the two composites also over the Indian Ocean indicates a warm SST anomaly observed over the north Indian Ocean during ELLA years whereas a cold SST anomaly is observed during LALA years. It is interesting to see whether such differences in SST anomalies over the Indo-Pacific Ocean during ELLA and LALA years have an influence on the ISMR variability which is analyzed in the next section.

3.2 Comparison of rainfall over India for ELLA and LALA events

We analyzed the composites of percentage rainfall anomaly patterns during the JJAS season over the Indian region corresponding to the ELLA and LALA years (Fig. 2a and 2b). We found that

during ELLA (Fig. 2a), the ISMR is characterized by significant positive rainfall anomalies over peninsular India, west-central India, north-western India, and some parts of north-eastern India. Negative percentage rainfall anomalies are found over parts of the Indo-Gangetic plains. On the contrary, the LALA composite (Fig. 2b) is characterized by a significantly negative percentage rainfall anomaly over northern parts of peninsular India, southern parts of central India, and parts of western India, especially near the Gujarat region. Positive percentage rainfall anomaly values are found over the north-central and Indo-Gangetic plains. This spatial distribution of rainfall anomaly indicates that India receives above-normal rainfall over many regions of the country during ELLA years, as compared to LALA years (Fig. 2a and b). It was also seen that India as a whole on average received about 9% above normal rainfall during ELLA composite years compared to only about 1% above normal rainfall during the LALA composite, as per the India Meteorological Department (IMD) observed ISMR data. It was also interesting to note that the western parts of India (Indo-Gangetic plains) receive above (below) normal rainfall during ELLA (LALA) years (Fig. 2a and b). It is now interesting to see the circulation patterns that controls the asymmetry in the rainfall behaviors over India during ELLA and LALA years.

3.3 Large-scale circulation over the Indo-Pacific region

We have examined the composite of moisture divergence and transport at 850 hPa during the JJAS season over Indian regions for ELLA and LALA years and presented in Fig 2c and 2d. The low-level westerly winds over the warm Arabian Sea and the north Indian Ocean is conducive to bring moist air from the Indian Ocean to the Indian landmass contributes to rainfall over India((Behera and Ratnam, 2018; Ratna et al. 2015). As seen in Figure 2c, for the ELLA composite, the south-westerly flow of the moisture flux transport is clearly visible, taking moisture supply to the western parts of India; which causes the moisture convergence and hence positive values of the percentage rainfall anomaly over these areas (Fig. 2a). However, during the LALA composite (Fig. 2d), the south-westerly moisture supply to India is reduced compared to the ELLA composite and there is zone of moisture divergence over western parts India contributing to below normal rainfall. At the same time, a significant value of moisture flux convergence over the Indo-Gangetic plains contributed to the above-normal rainfall during the LALA years (Fig. 2b).

To understand the mechanism and large-scale circulation responsible for the asymmetry in the rainfall pattern over India for ELLA and LALA composites during the monsoon season, we analyzed the velocity potential (shaded) along with the divergent wind (vector) at the upper-level (200 hPa) of the atmosphere in figure 3a and figure 3b. In the ELLA composite (Fig. 3a), strong convergent of wind vectors and positive values of the velocity potential anomaly are seen over the central Pacific Ocean. The upper-level divergent wind vectors and negative velocity potential anomaly are present over the Maritime continent, the Indian Ocean, and the Indian landmass associated with warm SST anomaly over the region (Fig. 2d). This indicates a low-level convergence and strong convection that represents in terms of rainfall anomaly over India in the ELLA composite (Fig. 2a).In the case of LALA composite (Fig. 3b), the converging wind vector and positive values of the velocity potential anomaly are still present over the central Pacific region but the magnitude, as well as the spread of these values, is reduced compared to the ELLA composite. At the same time, the divergent wind vector gets shifted southeastward and shows relatively weak negative values of the velocity potential over the western Pacific Ocean and Australia. This indicates that the upper-level divergence over the Indian landmass is reduced during LALA years and represents the weakening of low-level convergence over Indian landmass during LALA years compared to the ELLA years. This is coinciding well with the Indian landmass receiving less rainfall during LALA years compared to ELLA years (Fig. 2a and b).

Many observational studies show that the pressure oscillations and winds over the Indo-Pacific region can modulate the ISMR pattern up to a large extent (Walker, 1918; Ropelewski and Halpert, 1987; Hrudya, 2021, Ratna et al., 2021). To understand the ascending and descending motion over the tropical Indo-Pacific region and its contribution to the ISMR during ELLA and LALA composites; we analyzed the large-scale east-west tropical Walker circulation features over the Indo-Pacific region (Fig. 3c and Fig 3d). It was seen in the ELLA composite (Fig. 3c), a strong descending motion can be seen over the eastern and central Pacific Ocean whereas an ascending motion is seen over the Indian landmass and tropical Indian Ocean region (60 ^{o}E to 90 ^{o}E), a typical La Niña pattern. This ascending motion over the Indian region represents low-level convergence and enhanced convection contributes to more rainfall over India. However, this ascending motion over the Indian Ocean gets shifted eastward (near 120 ^{o}E) in the LALA composite (Fig. 3d), coincides with the eastward shift seen in the velocity potential and divergent winds (Fig. 3a and

Fig. 3b). This indicates that the low-level convergence and the rising motion over the Indian landmass region weakens and shifts southeastward reducing the convection and hence reducing the intensity of rainfall over India during LALA events.

4. Conclusion

In the present study, we examined the response of the Indian summer monsoon rainfall with respect to the two types of La Niña evolution by analyzing the composites of the SST, rainfall, the atmospheric circulation features using velocity potential, divergent wind anomalies, and the Walker circulation. We categorized the cold phase of the ENSO (La Niña) into two types based on the evolution of Niño 3.4 index in the Pacific Ocean. The La Niña condition in the summer monsoon (JJAS) season preceded by the El Niño (La Niña) condition in the previous boreal winter (DJF) season is termed ELLA (LALA). Based on the two types of La Niña evolution, we identified nine ELLA and eight LALA events during the period 1961-2021.

It was found that India received above-normal rainfall during the ELLA years compared to the LALA years. Spatial distribution of the rainfall anomaly for the JJAS season showed a significant positive value over most parts of India including peninsular India, central-western India, north-western India, and some parts of north-eastern India during ELLA years. Whereas during LALA, positive rainfall anomaly values are found only over the north-central and Indo-Gangetic plains. At the same time a significant negative percentage rainfall anomaly was present over western India, especially near the Gujarat region as well as northern parts of peninsula India. The comparison between the two rainfall composites indicated a significant reduction in the ISMR over the major parts of India during the LALA years compared to the ELLA years.

It was observed during the JJAS season that significant negative SST anomalies are present over the eastern and central Pacific Ocean for the ELLA events. Whereas significant positive SST anomalies in the western Pacific Ocean and the neighborhood of the Maritime continent. However, significant negative SST anomalies were present mostly over the central Pacific Ocean but with a weaker intensity during LALA events. This clearly indicated that SST anomalies over the tropical Indo-Pacific Ocean are different in terms of distribution and intensity for the ELLA and LALA years.

The dynamical analysis during the ELLA composite indicates a well-established moisture flux transport at the lower level (850 hPa) from the warm Arabian Sea towards India and causing moisture convergence over western parts of India. This moisture convergence over the western India region is contributing to the above-normal rainfall. However, during LALA, the moisture transport from cold Arabian Sea was reduced towards India, and a zone of significant moisture flux divergence was observed over western India, thereby contributing to the negative rainfall anomaly over central-western India. Further analysis of large-scale circulation indicates, an upper-level divergence represents a low-level convergence and enhanced convection over the Indian landmass contributing to above normal rainfall during ELLA years. In the case of LALA, the weak or absence of upper-level divergence over Indian landmass indicates the weakening of low-level convergence over the Indian landmass and hence the reduction of the ISMR.

In conclusion, the low-level convergence and enhanced rising motion over the Indian landmass contribute to the enhanced convection and the above-normal rainfall over India during ELLA years. However, the low-level convergence and the rising motion over the Indian region weakens and shifts southeastward, reducing the convection and hence reducing the intensity of rainfall over India during LALA years. Many earlier studies showed a well-established inverse relationship between the La Niña and the ISMR (Sikka and Gadgil, 1980; Webster and Yang, 1992; Samanta et al., 2020; Sharma et al., 2023). However, the present study concluded how different types of La Niña evolution contributed to the difference in the rainfall distribution for the Indian summer monsoon by modulating the large-scale atmospheric circulation and the monsoon winds over the tropical Indo-Pacific Ocean. This study will be helpful for better understanding of the distribution and intensity of rainfall anomaly over India based on the evolution of the SST anomaly in the equatorial Pacific Ocean.

Acknowledgments

The authors are thankful to the Head, of Climate Research and Services India Meteorological Department, Pune for the support and necessary facilities to pursue this study. Tanu Sharma acknowledges the research fellowship support from the MRFP (Ministry of Earth Sciences Research Fellowship Program) Project, MoES, Government of India. The authors also acknowledge DGM, IMD for necessary support.

Conflict of Interest

The authors declare no conflicts of interest relevant to this study.

Open Research

The data used in this study can be downloaded from the following websites: Oceanic Niño Index (ONI) data available at https://origin.cpc.ncep.noaa.gov/products/analysis_monitoring/ensostuff/ONI_v5.php; rainfall data prepared by the India Meteorological Department (Pai et al., 2014) available at https://www.imdpune.gov.in/cmpg/Griddata/Rainfall_25_NetCDF.html; Extended Reconstructed Sea monthly Surface Temperature (ERSST, Huang et al., 2017) available at https://psl.noaa.gov/data/gridded/data.noaa.ersst.v5.html; horizontal wind velocity components (u, v) and vertical wind velocity (w) are used from NCEP-NCAR Reanalysis 1 (Kalnay et al., 1996) available at https://psl.noaa.gov/data/gridded/data.ncep.reanalysis.html

References

Behera, S. K., & Ratnam, J. V. (2018). Quasi-asymmetric response of the Indian summer monsoon rainfall to opposite phases of the IOD. Scientific Reports, 8, 123. https://doi.org/10.1038/s41598-017-18396-6

Chakraborty, A., & Singhai, P. (2021). Asymmetric response of the Indian summer monsoon to positive and negative phases of major tropical climate patterns. *Nature Scientific Reports*, 11:22561, 1-13. https://doi.org/10.1038/s41598-021-01758-6

Cole, J. E. (2002). Multiyear La Niña events and persistent drought in the contiguous United States. *Geophysical Research Letters*, 29, 1-4. https://doi.org/10.1029/2001GL013561

Cherchi, A., Terray, P., Ratna, S. B., Sankar, S., Sooraj, K. P., and Behera, S. (2021). Chapter 8 - Indian Ocean Dipole influence on Indian summer monsoon and ENSO: A review, Indian Summer Monsoon Variability. *Elsevier*, ISBN 9780128224021, 157-182. https://doi.org/10.1016/B978-0-12-822402-1.00011-9

Collins, M., An, S. I., & Cai, W. e. a. (2010). The impact of global warming on the tropical Pacific Ocean and El Niño. *Nature Geoscience*, 3, 391–397. https://doi.org/10.1038/ngeo868

Dommenget, D., Bayr, T., & Frauen, C. (2013). Analysis of the non-linearity in the pattern and time evolution of El Niño southern oscillation. *Climate Dynamics*, 40, 2825–2847. https://doi.org/10.1007/s00382-012-1475-0

Gadgil, S., & Gadgil, S. (2006). The Indian monsoon, GDP and agriculture. *Economic and Political Weekly*, 41, 4887–4895.

Gadgil, S., Rajeevan M. and Francis P. A. (2007). Monsoon variability: links to major oscillations over the equatorial Pacific and Indian oceans. *Current Science*, 93, 182–94.

Gillett, N. P., Graf, H. F., & Osborn, T. J. (2003). Climate change and the North Atlantic oscillation. *Geophysical Monograph American Geophysical Union*, 134, 193–210. https://doi.org/10.1029/134GM09

Goswami, B. N. (2004). South Asian Summer Monsoon: An Overview; in the Global Monsoon System: Research and Forecast [Third International Workshop on Monsoon (IWM-III) (WMO TD 1266) (2-6 November)]. http://www.wmo.int/pages/prog/arep/tmrp/documentd/global_monsoon_system_IWM3.pdf.

Hrudya, P. H., Varikoden, H., & Vishnu, R. (2021). A review on the Indian summer monsoon rainfall, variability and its association with ENSO and IOD. *Meteorology and Atmospheric Physics*, 133, 1-14. https://doi.org/10.1007/s00703-020-00734-5

Huang, B., & Peter, W. et. al. (2017). Extended Reconstructed Sea Surface Temperature version 5 (ERSSTv5), Upgrades, validations, and intercomparisons. *Journal of Climate*, 30, 8179-8205. https://doi.org/10.1175/JCLI-D-16-0836.1

Iwakiri, T., & Watanabe, M. (2021). Mechanisms linking multi-year La Niña with preceding strong El Niño. *Scientific Reports*, 11, 17465. https://doi.org/10.1038/s41598-021-96056-6

Jin, F. F., Neelin, J. D., & Ghil, M. E. (1994). El Niño on the devil's staircase: Annual subharmonic steps to chaos. *Science*, *264*, 70-72. https://www.science.org/doi/10.1126/science.264.5155.70

Kalnay, E., Kanamitsu, M., Kistler, R., Collins, W., Deaven, D., Gandin, L., Iredell, M., Saha, S., White, G., Woollen, J., & Zhu, Y. (1996). The NCEP/NCAR 40–issued reanalysis project. *Bulletin of the American Meteorological Society*, *77*, 437–472. https://doi.org/10.1175/1520-0477(1996)077<0437:TNYRP>2.0.CO;2

Krishna Kumar, E. K., Abhilash, S., Syam, S., Vijaykumar, P., Santosh, K. R., & Sreenath, A. V. (2023). Contrasting Regional Responses of Indian Summer Monsoon Rainfall to Exhausted Spring and Concurrently Emerging Summer El Niño Events. *Advances in Atmospheric Sciences.* https://doi.org/10.1007/s00376-022-2114-2

Kritman, B., & Shukla, J. (2000). Influence of the Indian summer monsoon on ENSO. *Quarterly Journal of the Royal Meteorological Society*, 126, 213–239. https://doi.org/10.1002/qj.49712656211

Kumar, K. K., Rajagopalan, B., & Cane, M. A. (1999). On the Weakening Relationship Between the Indian Monsoon and ENSO. *Science*, 284(5423), 2156-2159. https://www.science.org/doi/10.1126/science.284.5423.2156

Neelin, J. D., Jin, F. F., & Syu, H. H. (2000). Variations in ENSO phase locking. *Journal of Climate*, 13, 2570–2590. https://doi.org/10.1175/1520-0442(2000)013<2570:VIEPL>2.0.CO;2

Pai, D. S. (2004). A possible mechanism for the weakening of El Nino-monsoon relationship during the recent decades. *Meteorology and Atmospheric Physics*, 86, 143-157. https://doi.org/10.1007/s00703-003-0608-8

Pai, D. S., Sridhar, L., Rajeevan, M., Sreejith, O. P., & Mukhopadhyay, B. (2014). Development of a new high spatial resolution (0.25° X 0.25°) Long period (1901-2010) daily gridded rainfall data set over India and its comparison with existing data sets over the region. *Mausam*, 65, 1-18. https://doi.org/10.54302/mausam.v65i1.851

Rasmusson, E. M., & Carpenter, T. H. (1983). The Relationship Between Eastern Equatorial Pacific Sea Surface Temperatures and Rainfall over India and Sri Lanka. *Monthly Weather Review*, 111, 517-528. https://doi.org/10.1175/1520-0493(1983)111<0517:TRBEEP>2.0.CO;2

Ratna, S. B., Cherchi, A., Osborn, T. J., Joshi, M., & Uppara, U. (2021). The Extreme Positive Indian Ocean Dipole of 2019 and Associated Indian Summer Monsoon Rainfall Response. *Geophysical Research Letters*, 48, 1-11. https://doi.org/10.1029/2020GL091497

Ratna, S.B., Cherchi, A., Joseph, P.V., Behera, S. K., Abish, B., Masina, S. (2015). Moisture variability over the Indo-Pacific region and its influence on the Indian summer monsoon rainfall. Climate Dynamics 46, 949–965. https://doi.org/10.1007/s00382-015-2624-z

Ropelewski, C. F., & Halpert, M. S. (1987). Global and Regional Scale Precipitation Patterns Associated with the El Niño/Southern Oscillation. *Monthly Weather Review*, 115, 1606-1626. https://doi.org/10.1175/1520-0493(1987)115<1606:GARSPP>2.0.CO;2

Roxy, M. K., & Chaithra, S. T. (2018). Climate Change and Water Resources in India.Chapter 2: Impacts of Climate Change on the Indian Summer Monsoon. Ministry of Environment, Forest and Climate Change (MoEF & CC), Government of India. ISBN: 978-81-933131-6-9

Saji, N. H., Goswami, B. N., Vinayachandran, P. N., & Yamagata, T. (1999). A dipole mode in the tropical Indian Ocean. *Nature*, 401, 360-363. https://doi.org/10.1038/43854

Samanta, D., Rajagopalan, B., Karnauskas, K. B., Zhang, L., & Goodkin, N. F. (2020). La Niña's diminishing fingerprint on the central Indian summer monsoon. Geophysical Research Letters, 47, e2019GL086237. https://doi.org/10.1029/2019GL086237

Sharma, T., Ratna, S. B., Pai, D. S. (2023). Modulation of Indian Summer Monsoon Rainfall response to ENSO in the recent decades and its large-scale dynamics. PREPRINT (Version 1) available at Research Square [https://doi.org/10.21203/rs.3.rs-2405719/v1]

Shukla, R. P., & Haung, B. (2016). Interannual variability of the Indian summer monsoon associated with the air-sea feedback in the northern Indian Ocean. *Climate Dynamics*, 46, 1977–1990. https://doi.org/10.1007/s00382-015-2687-x

Sikka, D. R., & Gadgil, S. (1980). On the maximum cloud zone and the ITCZ over Indian longitudes during the southwest monsoon. *Monthly Weather Review*, 108, 1840-1853. https://doi.org/10.1175/1520-0493(1980)108<1840:OTMCZA>2.0.CO;2

Timmermann, A., An, S. I., & Kug, J. S. e. a. (2018). El Niño–Southern Oscillation complexity. *Nature*, 559, 535–545. https://doi.org/10.1038/s41586-018-0252-6

Tziperman, E., Stone, L., Cane, M. A., & Jarosh, H. E. (1994). El Nino chaos: Overlapping of resonances between the seasonal cycle and the Pacific ocean-atmosphere oscillator. *Science*, *264*, 72-74. https://www.science.org/doi/10.1126/science.264.5155.72

Walker, G. T. (1918). Correlation in seasonal variation of weather. *Quarterly Journal of the Royal Meteorological Society*, 44, 223-224.

Webster, P. J., & Yang, S. (1992). Monsoon and ENSO: Selectively interactive systems. *Quarterly Journal of the Royal Meteorological Society*, 118(507), 877–926. https://doi.org/10.1002/qj.49711850705

Zhang, R. H., Gao, C., & Feng, L. (2022). Recent ENSO evolution and its real-time prediction challenges. *National Science Review*, 9. https://doi.org/10.1093/nsr/nwac052

Figures:

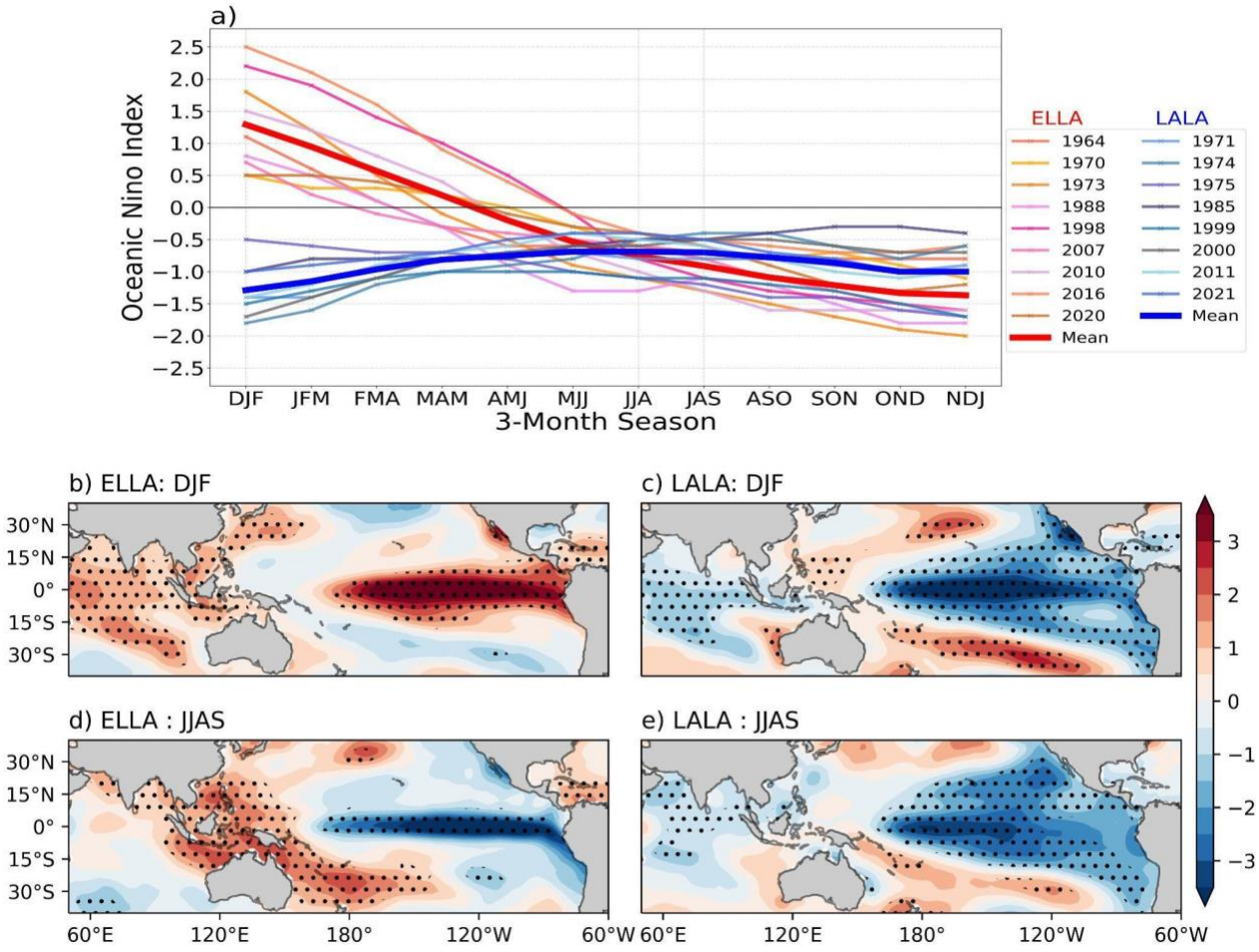

Figure 1. a) Three-month season time series of Oceanic Niño Index (ONI) for ELLA (La Niña preceded by El Niño) and LALA (La Niña preceded by La Niña) years between 1961 to 2021. The mean ONI for ELLA and LALA years is represented by red and blue thick lines respectively. Detrended SST anomaly composites for **b)** ELLA (DJF) **d)** ELLA (JJAS) years. **c)** and **e)** are the same as b) and d) but for LALA years. Dotted marks (b – e) are significant values at the 90% confidence level based on the Student's t-test. For the anomaly calculation, 1961-2020 climatology is considered.

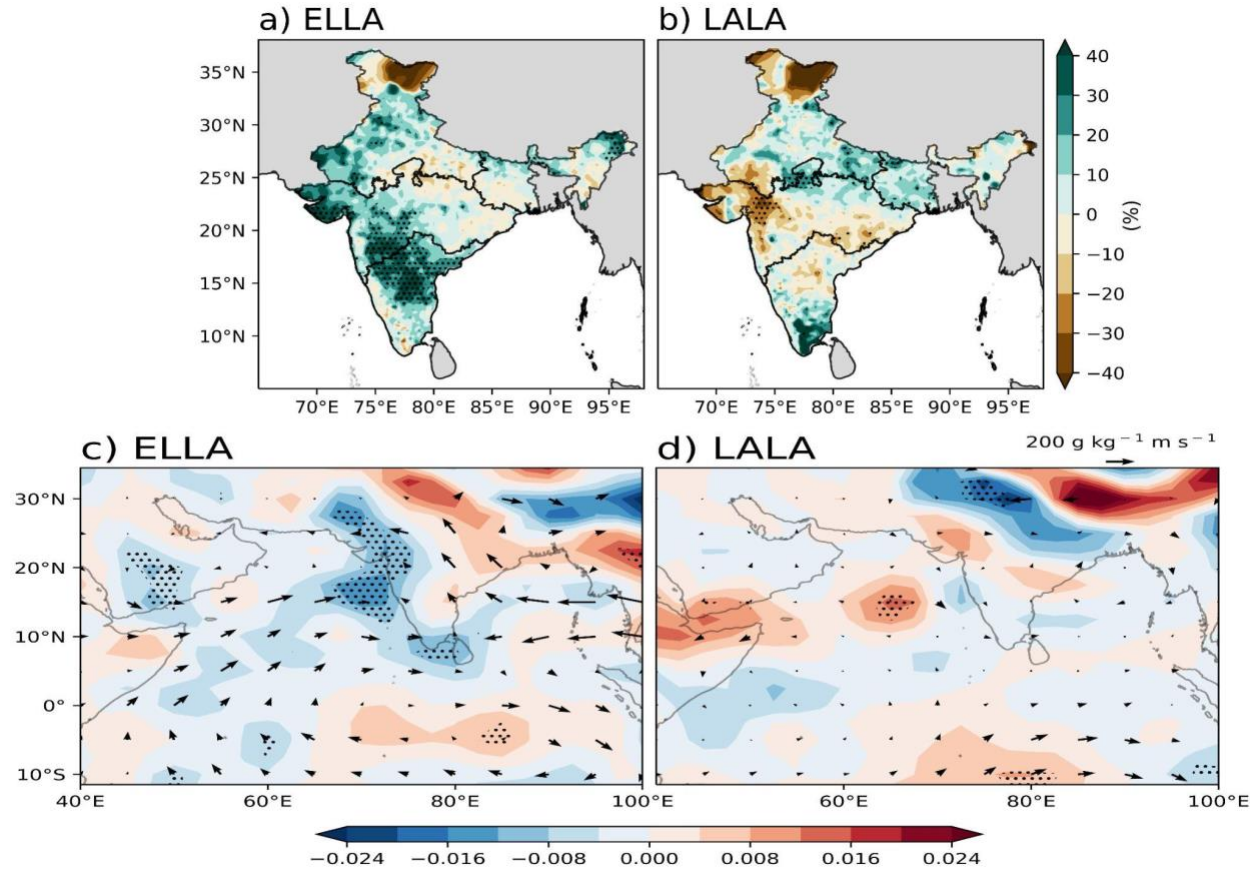

Figure 2. Percentage seasonal rainfall anomaly (June-September) composites for **a)** ELLA and **b)** LALA years. **c)** and **d)** are the same as a) and (b) but for moisture flux divergence (shaded, 10^2 s^{-1}) overlaid with moisture flux transport vector (g kg^{-1} m s^{-1}) at 850 hPa. Dotted marks are significant values at the 90% confidence level based on the Student's t-test. For the anomaly calculation, 1961-2020 climatology is considered.

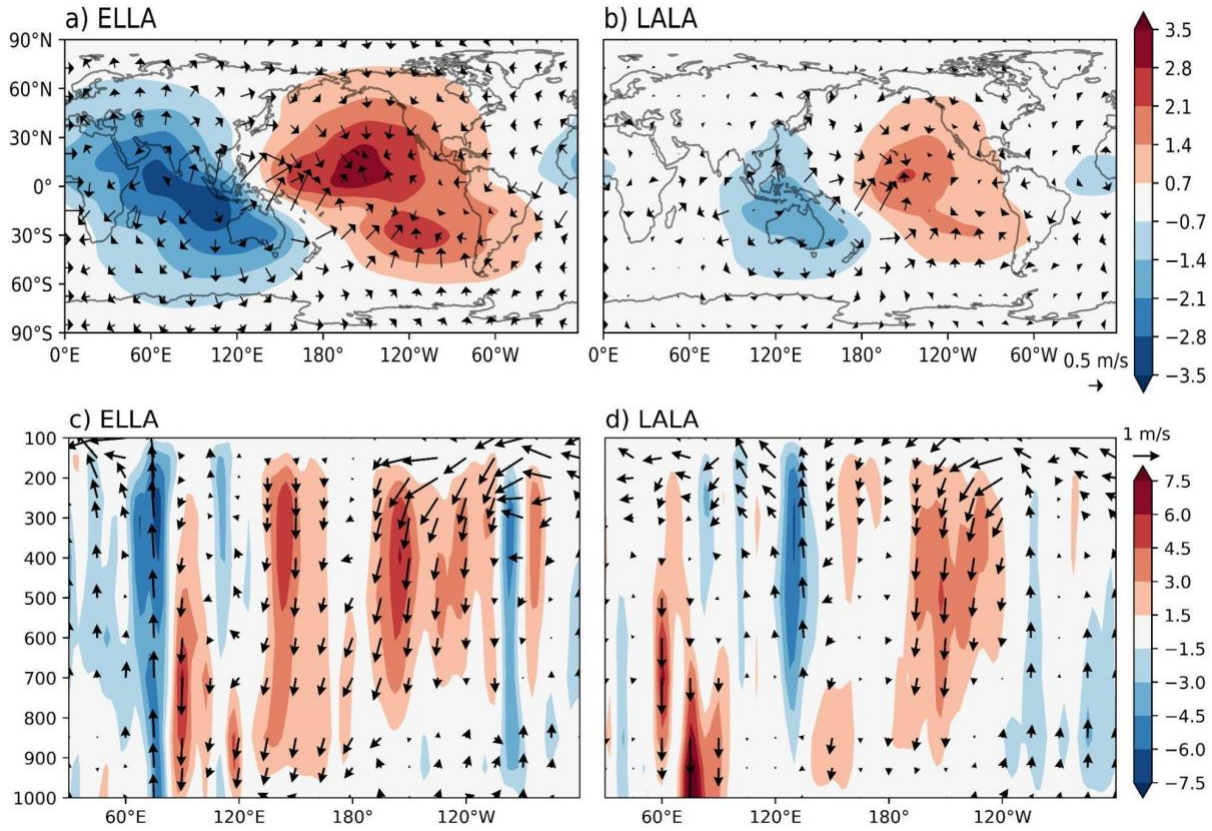

Figure 3. Velocity potential anomaly composite (shaded, $10^6 \times m^2\ s^{-1}$) along with the divergent wind (vector) at 200 hPa for **a)** ELLA and **b)** LALA years. Walker circulation anomalies over the Indo-Pacific sector for **c)** ELLA and **d)** LALA years. In c) and d) vector has zonal (u) and vertical (w) wind components, from 1000 hPa to 100 hPa pressure level and values are averaged over latitude 7.5 ºN - 37.5 ºN. Color contour representing $w \times 10^3\ m\ s^{-1}$.